

CrossMark
click for updatesCite this: *Chem. Sci.*, 2014, 5, 3355

The right touch: design of artificial antigen-presenting cells to stimulate the immune system

Joep van der Weijden,^{†a} Leonie E. Paulis,^{†b} Martijn Verdoes,^{ab} Jan C. M. van Hest^a and Carl G. Figdor^{*b}

With the ever expanding possibilities to build supramolecular structures, chemists are challenged to mimic nature including the construction of artificial cells or functions thereof. Within the field of immunology, effective immunotherapy critically depends on efficient production of antigen-specific cytotoxic T-cells. Herein lies an opportunity for chemists to design and synthesize so-called artificial antigen presenting cells (aAPCs) that can promote T-cell activation and their subsequent expansion. In this review we discuss the current status of aAPC development, also focusing on developments in nanoscience which might improve future designs. As synthetic mimics of natural antigen-presenting cells, aAPCs encompass three basic signals required for T-cell activation: MHC–antigen complexes, costimulatory molecules and soluble immune modulating compounds. Both spatial and temporal organization of these signals during aAPC/T-cell contact is important for efficient T-cell activation. We discuss how signals have been incorporated in several aAPC designs, but also how physical properties such as size and shape are essential for targeting the aAPCs to T-cell rich areas *in vivo*.

Received 15th April 2014
Accepted 22nd May 2014

DOI: 10.1039/c4sc01112k

www.rsc.org/chemicalscience

Introduction to cancer immunotherapy

One of the most promising advances in the global fight against cancer is the development of immune-mediated anti-cancer therapies.¹ Cancer immunotherapy is aimed at training the immune system such that cancer cells are selectively recognized and destroyed based on tumor antigens expressed on their cell membrane. Based on this specificity, successful implementation of cancer immunotherapy has many benefits over existing therapies, especially the development of long-lived immunity against cancer in the absence of major side effects.

Key players in the immune system are antigen presenting cells (APCs), in particular dendritic cells (DCs), which are considered the master organizers of the immune system. When DCs encounter tumor tissue, they pick up antigenic fragments of the tumor cells, and are stimulated to migrate to the lymphoid organs (*i.e.* lymph nodes and spleen) for antigen presentation to T-cells. DCs process the captured tumor antigens into small peptide fragments of 9–12 amino acids long and present these embedded in so called major histocompatibility complex (MHC) class I and II proteins expressed on their cell surface. Subsequently, T-cells recognize these MHC–antigen complexes on DCs *via* their T-cell

receptors (TCRs). Importantly, two types of MHC class I and II proteins interact with different T-cell subsets, being CD8⁺ and CD4⁺ T-cells, respectively. Upon simultaneous presentation of costimulatory signals by DCs, T-cells will acquire an activated phenotype and will proliferate. CD8⁺ T-cells develop into cytotoxic effector cells capable of rapid and efficient killing of antigen expressing cells (*i.e.* tumor cells), whereas CD4⁺ T-cells differentiate into helper cells that sustain an active anti-tumor response *via* cytokine secretion.² To create a strong instantaneous immune response, T-cells with an effector phenotype are produced and released into the body to perform their function, *i.e.* killing of tumor cells, after migration into the tissues where tumor resides.

Unfortunately, in many cancer patients, the endogenous immune response towards tumor cells is severely impaired, because cancer antigens mainly consist of self-antigens which lack the power to provoke a strong immune response. To boost the anti-tumor immune response, two different cell-based approaches have evolved: DC vaccination and adoptive T-cell transfer (Fig. 1). Both treatments rely on the re-infusion of *ex vivo* stimulated patient-derived autologous immune cells. The first approach is aimed at the *ex vivo* loading of DCs with tumor antigens and costimulatory molecules. Upon administration of these DCs to patients, they are thought to migrate to the lymph nodes to actively stimulate tumor-specific T-cells. The alternative approach focuses on the *ex vivo* production of tumor-specific T-cells from blood or tumor biopsies, thereby providing patients directly with tumor-cytotoxic T-cells.^{3–5}

During the past 15 years, early clinical trials have been performed using both DC vaccination and adoptive T-cell

^aRadboud University Nijmegen, Institute for Molecules and Materials, Heyendaalseweg 135, 6525 AJ Nijmegen, The Netherlands. E-mail: j.vanhest@science.ru.nl; Fax: +31 243653393; Tel: +31 243653204

^bRadboud Institute for Molecular Life Sciences, Radboud University Medical Center, Geert Grooteplein 26-28, 6525 GA Nijmegen, The Netherlands. E-mail: C.Figdor@ncmls.ru.nl; Fax: +31 243540339; Tel: +31 1243617600

[†] These authors contributed equally to this work

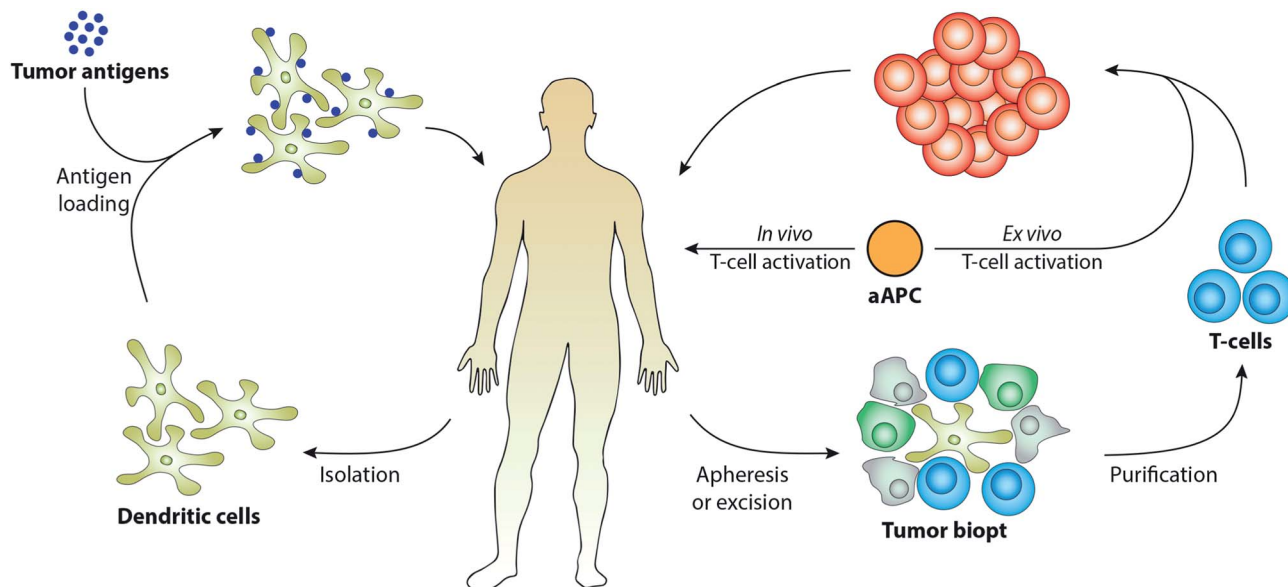


Fig. 1 Outline of DC vaccination and adoptive cell transfer for the treatment of cancer. In DC vaccination, autologous DCs are harvested and loaded with antigens *ex vivo*, and then re-infused for treatment. In adoptive T-cell transfer, tumor-antigen specific T-cells are harvested and isolated from a tumor biopt, stimulated with either soluble antibodies or first generation aAPCs *ex vivo* and finally re-infused for treatment. Alternatively, direct injection of second generation aAPCs can allow for *in vivo* stimulation of tumor-antigen specific T-cells, circumventing *ex vivo* cell handling procedures.

transfer.^{2,4-6} However, their wide-spread clinical use remains limited as implementation is very laborious and costly, particularly because the cells that are used for treatment have to be derived and processed from individual patients.³ This means that for every patient a tailor made product must be made. Other cancer immunotherapies that have been developed, such as cytokine or antibody treatment (*e.g.* trastuzumab, rituximab) temporarily boost the immune system. Although these products can be made in large quantities and can be applied to large groups of patients as opposed to cell-based approaches, they usually lack the ability to produce a memory type of immune response and therefore require repeated treatments at short intervals.

Cancer immunotherapy could therefore greatly benefit from the development of fully synthetic DC analogues, as an 'off-the-shelf' product to elicit highly reproducible antigen-specific immune responses upon administration into patients *via in vivo* direct T-cell activation. This has led to the production of so-called artificial antigen-presenting cells (aAPCs). The development of such off-the-shelf aAPCs that can be directly injected into patients would circumvent *ex vivo* cell handling procedures, resulting in a more cost-effective immune therapy with the additional advantage of offering a high degree of control over the ultimate immune response.

Not only basic scaffold design parameters such as size, shape and rigidity are important to capture the complexity of natural T-cell activation with synthetic constructs. Other factors must also be carefully tuned, such as the mobility of T-cell activating ligands to closely mimic natural signal transduction or the controlled release of cytokines from aAPCs to direct T-cell differentiation.

In this review we will first briefly describe the biology involved in natural T-cell activation and continue with a discussion on recent progress made within in the field of aAPC design. Special emphasis is given on aspects essential for *in vivo* T-cell activation by aAPCs.

Requirements for biomimetic T-cell activation

The concept of artificial antigen presentation on micro- or nanoparticles was already introduced in the late 1970s (ref. 7) and ever since, a wide variety of biomaterials have been proposed as a scaffold for aAPCs.⁸ Recent advances in biomaterial science have enabled researchers to translate immunological knowledge into biomimetic material properties. Two immunological aspects are particularly relevant for aAPC design, being the basic signaling components required for T-cell activation, and the spatial and temporal organization of these signaling components on the aAPC scaffold.

Signaling components

Activation of T-cells by DCs requires three basic signals, as illustrated in Fig. 2A. The first signal (signal 1) is obtained from the recognition of MHC-antigen complexes on DCs by TCRs on the T-cell. The affinity of a TCR for a single MHC-antigen complex is rather low ($K_d = 1-100 \mu\text{M}$) and therefore, several MHC-TCR complexes are required to effectively stimulate T-cells. Importantly, the formation of MHC-TCR microclusters creates a synergistic enhancement of overall DC/T-cell binding through an increase in avidity.⁹ Membrane-bound adhesive

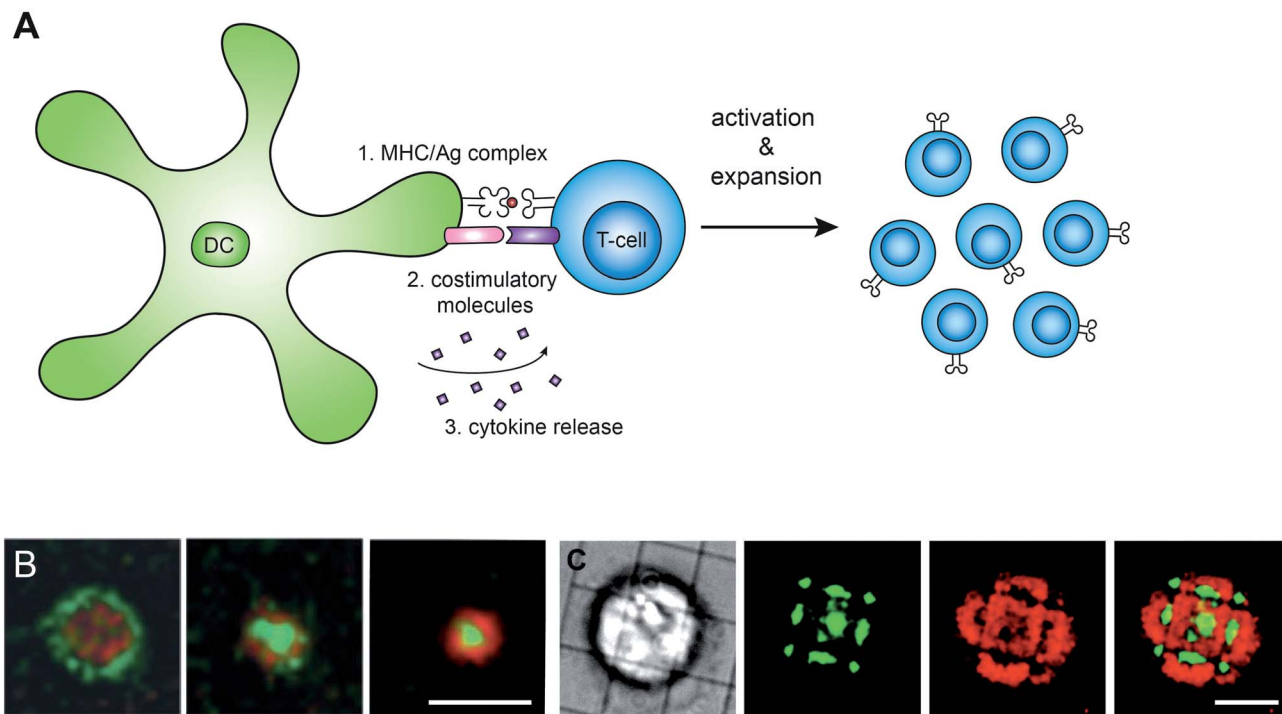


Fig. 2 (A) Schematic overview of DC signals required for T-cell activation. (1) MHC I/II–antigen complexes, (2) co-stimulatory or adhesive molecules, (3) cytokines. (B) Kinetics of IS formation on a T-cell binding a lipid bilayer showing the formation of the cSMAC and pSMAC. Green = MHC–complex, red = ICAM-1. Bar = 10 μm .¹⁷ From ref. 17. Reprinted with permission from AAAS. (C) Physical barriers to protein transport on a lipid bilayer created by thin chrome lines hamper the spatial organization of the IS. Green = TCRs, red = ICAM-1. Bar = 5 μm .²² From ref. 22. Reproduced with permission from AAAS.

proteins, such as the T-cell bound integrin LFA-1, surrounding these microclusters stabilize and prolong DC/T-cell interactions.^{10–12} As a result, a limited number of activating MHC–TCR complexes can be sufficient to trigger T-cells.^{9,13} To test the efficacy of aAPCs, antibodies against the TCR co-receptor CD3 are often used as a simple alternative recognition signal instead of using the more elaborate MHC–antigen complexes. Contrary to MHC–antigen complexes, which can only stimulate antigen-specific T-cells, anti-CD3 bypasses the antigen specific TCR derived signal by directly stimulating the cellular signaling machinery downstream of CD3.^{14,15} As a result, such anti-CD3 induced T-cell activation is non-specific and polyclonal (essentially all T cells are activated).

The second signal (signal 2) is provided by costimulatory membrane bound proteins on the DC, such as CD80, CD86 or 4-1BB ligand.² Both CD80 and CD86 interact with CD28, whereas 4-1BB ligand binds to 4-1BB. Both CD28 and 4-1BB are transmembrane signaling receptors on T-cells that upon binding to their ligands on DCs enhance the strength of the T-cell response to MHC–antigen complexes, which is especially valuable for weak affinity antigens.¹⁰ T-cell activation without co-stimulation through the CD28 receptor can lead to a state in which the T cell is anergic, *i.e.* meaning that it fails to respond after it reencounters its specific antigen.

The third signal (signal 3) comes from soluble signaling molecules, known as cytokines, which are secreted from DCs. A subset of immune modulating cytokines, named interleukins

(IL) is critical for T-cell polarization and subsequent differentiation into various phenotypes. For CD4⁺ T-cells in particular, this depends on the delicate balance between immune activating interleukins (*e.g.* IL-2, IL-15), and immunosuppressive interleukins (*e.g.* IL-10).^{2,16} The controlled release of interleukins from aAPCs is therefore crucial in order to fine-tune the immune response.

Immune synapse formation for optimal cell signaling

Dynamic microscopy of the interface between an APC and a T cell revealed the presence of a highly organized microdomain (5–10 μm), designated as the immune synapse (IS).^{11,17} The formation of this synapse is orchestrated by T-cells and is initiated by contact with APCs. To gain more insight in the dynamics and functional consequences of IS organization, supported lipid bilayers (SLBs) have been used as 2D mimics of APCs. SLBs are formed by deposition of lipid bilayers onto glass slides, with lipid mobility being preserved within the bilayer.¹⁸ Upon incorporation of fluorescently labeled T-cell ligands that mimic APC engagement, IS formation can be followed by visualizing the redistribution of T-cell ligands upon T-cell binding.

Extensive studies with SLBs demonstrated that the immune synapse is not only a highly dynamic structure but also an extremely specialized structure, characterized by actin-mediated rearrangement of TCRs and LFA-1 microclusters (1.5 μm^2) within the T-cell membrane into segregated domains. The IS adopts a bull's eye pattern, composed of the central

supramolecular activation cluster (cSMAC), formed by TCRs, which is surrounded by a ring of adhesion molecules called the peripheral SMAC (pSMAC) (Fig. 2B).^{17,19-21} Importantly, the cSMAC predominantly contains TCRs which have engaged MHC proteins, whereas non-bound TCRs reside within the pSMAC area.⁹

Of course, diffusion constants of T-cell ligands measured in SLBs are much higher than those in the cellular membrane, because lipid movement is not restricted by cytoskeletal anchors. Therefore, IS formation *via* SLBs might not accurately capture the dynamics of natural IS formation. To gain more insight in the effect of T-cell ligand mobility on T-cell activation, ligand micropatterns were created by introducing constraints to the lateral mobility of lipid-tethered ligands, or by immobilizing ligands onto a surface.²²⁻²⁴ These studies show that T-cell activation is severely hampered when ligands are physically hindered to rearrange into an IS (Fig. 2C). Recently, Hsu *et al.* developed a more physiologically relevant SLB with tunable lipid diffusion rates, using mixtures of lipids with different phase transition temperatures, and confirmed that a decreased lipid fluidity negatively affects the T-cell response.²⁵ These studies indicate that static ligand/receptor binding between aAPCs and T-cells is likely not sufficient for efficient T-cell

activation, and stress the importance of T-cell ligand mobility on aAPCs to allow for dynamic IS formation and efficient downstream signaling.

As the field of optical imaging progresses, super-resolution microscopy techniques such as photoactivated localization microscopy (PALM) and stochastic optical reconstruction microscopy (STORM) allow for the imaging of the IS at sub 100 nm resolution.²⁶ These techniques are becoming more accessible to immunologists and chemists alike, adding valuable information to our current knowledge about the immune synapse.

First generation aAPCs for *ex vivo* expansion of T-cells

In an attempt to develop a standardized platform for *ex vivo* tumor-specific T-cell expansion for cancer immune therapy, researchers developed a first generation of aAPCs, which were mainly based on solid, micron-sized polystyrene beads coated with T-cell ligands (Fig. 3).²⁷ These microparticles provided a large contact area between individual aAPCs and T-cells. In addition, they can be homogeneously dispersed with T-cells, which was shown to be a distinct advantage compared to 2D

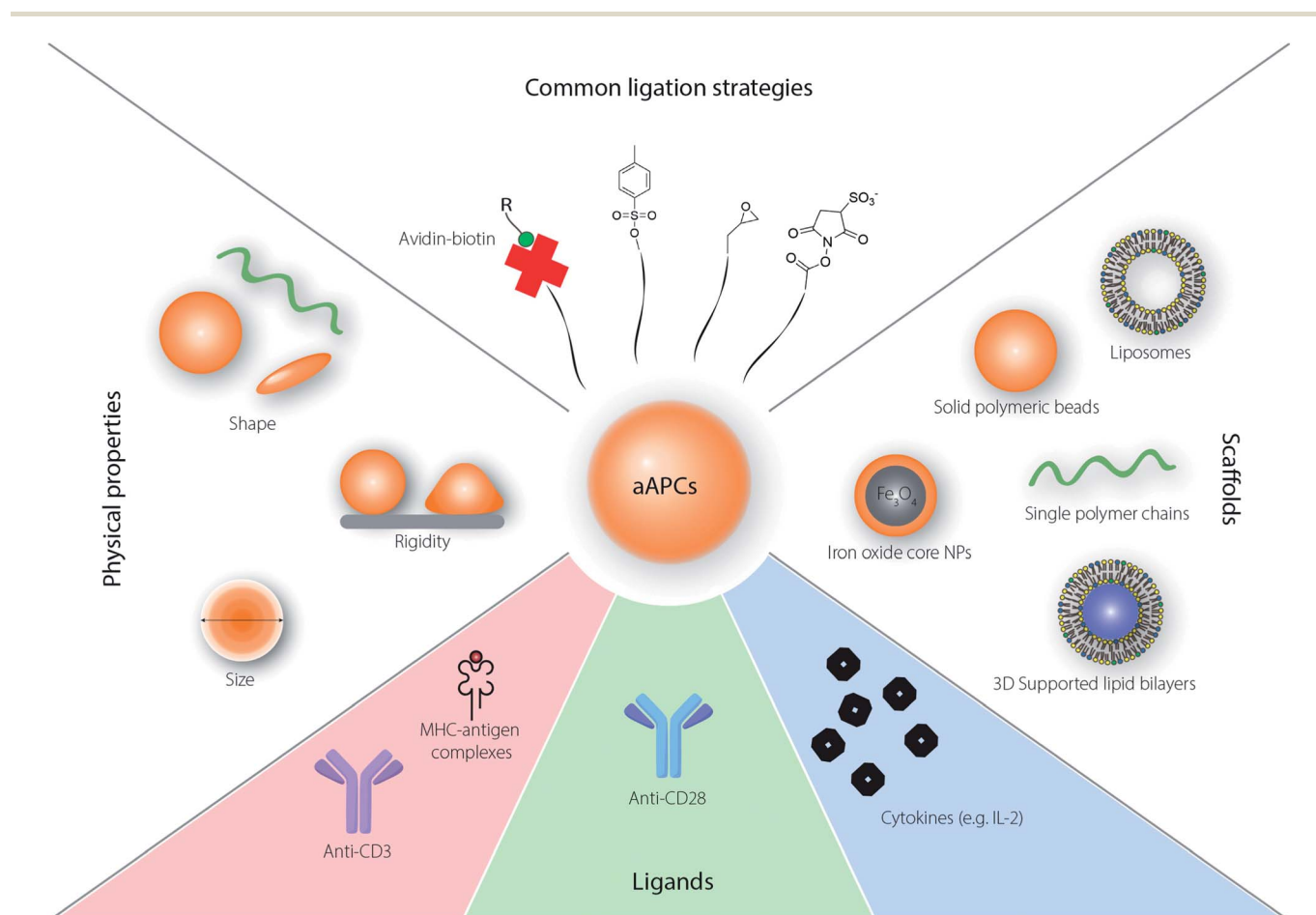


Fig. 3 Tunable biological, physical and chemical properties of artificial antigen presenting cells, which together determine their efficacy for T-cell activation. The most commonly used scaffolds, ligation chemistries and ligands are shown.

surfaces.²⁸ Initially, solid polystyrene (PS) beads were used as a scaffold material, prepared *via* controlled emulsion polymerization.²⁹ However, being a non-degradable polymer, PS has limited clinical potential. Therefore, a novel class of microparticles, so-called Dynabeads®, was developed, which are based on an iron oxide core coated with PS. The iron oxide core enables their easy magnetic removal from T-cells, making this system suited for safe *ex vivo* T-cell expansion for clinical application in adoptive T-cell transfer therapies.^{30–33}

T-cell ligands can be adsorbed onto these beads *via* non-covalent interactions or, alternatively, reactive tosyl-, or epoxide-groups can be incorporated, which allow for covalent attachment of ligands *via* reaction with nucleophilic amino acid side chains (Fig. 3).³⁴ Even though both PS and iron oxide-based beads completely lack ligand mobility to facilitate IS formation, they are very effective in *ex vivo* T-cell activation. They have been functionalized with costimulatory molecules in combination with either anti-CD3 antibodies to mimic polyclonal T-cell activation or MHC–antigen complexes to generate tumor-specific T-cells.^{34,35} Interestingly, bead-expanded T-cells showed multifunctional behavior, reflected in the secretion of various cytokines. Additionally, by using low densities of T-cell activating ligands, high avidity T-cells were selectively activated, resulting in very potent tumor-specific cytotoxic T-cells.³⁶

Various costimulatory molecules have been tested for their ability to boost either CD4⁺ or CD8⁺ T-cells.^{37–39} Deeths *et al.* observed that PS-based aAPCs prepared with CD80, which interacts with CD28 on T-cells, induced continuous CD4⁺ T-cell expansion, but only short-term CD8⁺ T-cell responses.⁴⁰ Antibodies against CD28 are commonly used as costimulatory molecules, since they are very effective at inducing IL-2 secretion which is important for T-cell expansion.³⁷ However, the type of T-cell response, as measured by cytokine secretion, may not be optimal when using anti-CD28. When focusing on CD8⁺ T-cells, a mix of CD28 and 4-1BB antibodies (1 : 3 ratio) was found to generate highest cytokine release.³⁹

The *in vivo* functionality of *ex vivo* bead-expanded T-cells has been tested in various models of adoptive T-cell transfer into tumor-bearing mice.^{41,42} In an elegant study, Durai *et al.* used immune-deficient SCID mice to prove that iron oxide bead-expanded human T-cells can elicit a potent immune response towards human melanoma tumors transplanted to these mice.⁴¹ As a next step, the capacity of beads to directly activate T-cells *in vivo* was explored.^{43–45} For this purpose, PS-beads coated with either melanoma-specific MHC I- or II-antigens together with costimulatory molecules were injected intravenously into mice, thereby aiming at CD8⁺ and CD4⁺ T-cell activation respectively.^{43,44} Both types of aAPCs were able to significantly delay tumor growth compared to beads that contained no tumor antigens but only costimulatory ligands. However, in both cases tumor growth could not be entirely prevented by aAPC treatment. In an *in vivo* setting, costimulatory molecules were essential to generate an efficient anti-tumor response, especially when using low affinity antigens, as was shown by Ugel *et al.* who used iron oxide beads coated with TRP-2 (a tumor antigen) combined with CD80.⁴⁵ However, micron-sized beads showed massive accumulation in the lungs, probably

reflecting the trapping of microparticles in lung capillaries. This might result in severe health risks, such as microvascular occlusion, which strongly limits the therapeutic potential of these systems.^{46,47}

Shifting towards aAPCs for *in vivo* T-cell activation

A crucial aspect in the design of aAPCs for *in vivo* applications, is their distribution in the body. Upon administration into patients, aAPCs should efficiently home to T-cell-rich areas, which are predominantly located in the lymph nodes and spleen. As biodistribution is largely dictated by the route of administration and particle properties such as size, morphology and stiffness, tuning these properties is crucial when targeting the lymphoid organs (Fig. 3).

In general, small particles (<100 nm) show the most dynamic behavior, due to their ability to pass through natural barriers in the body. For example, upon intradermal (skin) administration, small (25 nm) pluronic stabilized polypropylene (PPS) nanoparticles easily penetrated the extracellular matrix and by interstitial fluid pressure they rapidly moved towards skin-draining lymph nodes. This is in contrast to larger PPS particles (>500 nm), the majority of which remained physically stuck in the skin (Fig. 4A).^{48–51} Unfortunately, once in the lymph node, these PPS nanoparticles were prone to phagocytosis by *e.g.* macrophages, thereby rendering them unavailable for interacting with T-cells (Fig. 4B).⁴⁸ Particles can also be injected directly into the blood. Nanoparticles between 100–200 nm are optimally suited for prolonged circulation, which increases their time-window to accumulate in T-cell rich organs, since they are large enough to avoid uptake in the liver, but small enough to avoid filtration in the spleen.⁵² Larger particles (>200 nm) are rapidly filtered from the blood by macrophages in both the liver and spleen (Fig. 4C).^{46,47,53} Micron-sized particles are also trapped in the lungs, thereby blocking the local microvasculature.^{46,47}

Not only size, but also shape critically contributes to particle distribution in the body.^{47,54} Decuzzi *et al.* compared silica microparticles with a discoidal, spherical and cylindrical shape of similar volumes (0.6–0.8 μm^3) and found that disks showed lowest accumulation in the liver, whereas cylinders were least trapped in the lungs and spleen.⁴⁷ This was in agreement with Geng *et al.*, who showed that elongation of micelles into filamentous structures (8 μm length) significantly prolonged their circulation time, which might be explained by their ability to align with the blood flow.⁵⁵ In addition to particle geometry, the mechanical deformability also affects the biodistribution. Flexible particles are more easily deformed when passing through biological barriers.^{56,57} This was shown by Merkel *et al.*, who developed non-rigid microparticles with an elastic modulus ranging from 8–64 kPa, tuned by the degree of internal cross-linking. The circulation time was prolonged with decreasing stiffness, and moreover flexible particles were retained less in the lungs.⁵⁶

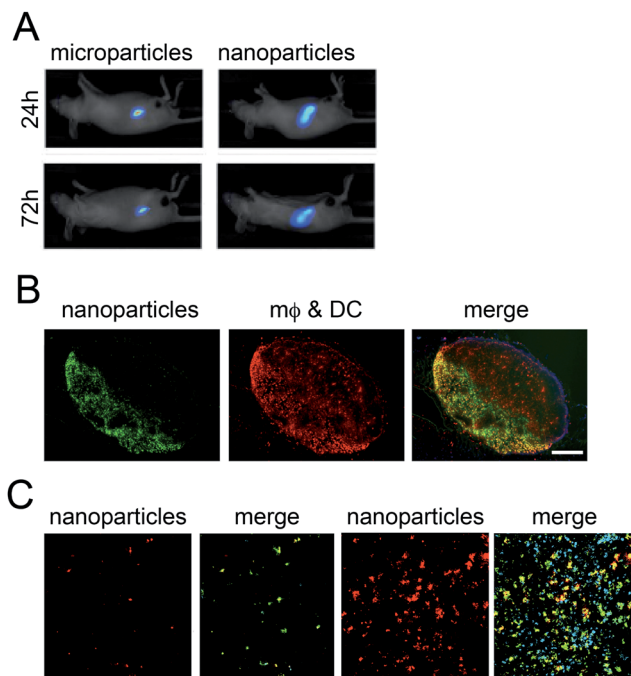


Fig. 4 (A) *In vivo* imaging of micron- and nano-sized aAPC (diameter 4.5 μm and 50–100 nm, respectively). Following subcutaneous injection, nanoparticles traffic from the migration site towards the inguinal lymph node within 24 h, whereas microparticles are physically stuck at the injection site.⁵⁰ Reprinted from *Nanomedicine*, 10, Perica *et al.*, Nanoscale artificial antigen presenting cells for T cell immunotherapy, 126, ©2014, with permission from Elsevier. (B) Within the lymph node, nanoparticles (20 nm) co-localize predominantly with phagocytic cells (*i.e.* macrophages and dendritic cells). Green = nanoparticles, red = CD68. Bar = 100 μm .⁴⁸ Reprinted from *Journal of Controlled Release*, 112, Reddy *et al.*, *In vivo* targeting of dendritic cells in lymph nodes with poly(propylene sulfide) nanoparticles, 29, copyright 2006, with permission from Elsevier. (C) Upon intravenous injection, nanoparticles (100 nm) predominantly accumulate in macrophages in the liver (left) and spleen (spleen) within 48 h. Red = nanoparticles, cyan = CD18, green = CD68. Bar = 100 μm .¹⁰⁶ Reprinted from *Journal of Controlled Release*, 162, Paulis *et al.*, Distribution of lipid-based nanoparticles to infarcted myocardium with potential application for MRI-monitored drug delivery, 281, copyright 2012, with permission from Elsevier.

As mentioned earlier, macrophage uptake of particles remains a problem irrespective of their size. To escape macrophage recognition, particles can be coated with hydrophilic polymers, such as FDA approved poly-(ethylene glycol) (PEG).^{58,59} PEGylation creates a hydrated layer on the particles' surface, thereby minimizing particle opsonization, a process which acts as a natural marker sign for phagocytosis by macrophages.⁴⁶ Alternatively, a small peptide derived from CD47 – which is a 'marker of self' membrane protein expressed by red blood cells, generating a 'don't eat me' signal – is a potentially interesting approach to prevent engulfment by macrophages and thereby enhance the circulation time of nanoparticles.⁶⁰

In conclusion, for *in vivo* applications of aAPCs, small nanoparticles (100 nm) display a favorable distribution towards T-cell-rich sites as the lymph nodes and spleen, even though

this size might not be ideally suited for T cell activation compared to microparticles. Alternatively, microparticles can be injected directly into the lymph node, thereby avoiding potential disadvantageous body distribution upon intradermal or intravenous injection.⁶¹

Adding complexity to design second generation aAPCs

To improve the performance of aAPCs for *in vivo* T-cell activation, a second generation of aAPCs is currently being developed. Due to recent advances in nanoscience, more complex micro- and nanoparticle architectures are now within reach, which allow for more detailed studies on the requirements for optimal T-cell activation.

Geometry

T-cell activation by DCs is a multi-phase process, in which the required DC/T-cell contact duration can last for more than one hour, depending on the activation stage of the T-cells.⁶² Therefore, to provide a platform for sustained signaling between aAPCs and T-cells, rapid internalization of aAPCs by T-cells should be prevented. As previously stated, the decision of cells to internalize particles depends, amongst others, on shape or rather local curvature, as it contacts the cell membrane. Consequently, increased resistance to phagocytosis might be obtained by carefully tuning particle shape.

To produce particles with non-spherical geometry, two different methods can be used: direct formation of non-spherical particles or deformation of pre-fabricated spherical particles.⁶³ The first approach encompasses, amongst others, photolithography and microfluidics, but the most popular and versatile technique is Particle Replication in Non-wetting Templates (PRiNT), which can produce any desired shape using nanoscale molds (Fig. 5A).⁶⁴ Using PRiNT technology, particles can be prepared from a huge variety of starting materials, including biocompatible compounds such as poly-(lactic-co-glycolic acid) (PLGA) or PEG. The second approach uses spherical solid particles, primarily composed of polymers such as PS or PLGA, whose shape can be modified by film-stretching of a thin sheath of particles.⁶⁵ Shape can be controlled by tuning the extent of film stretching and the time point of stretching (before or after liquefaction of the particles) (Fig. 5B). Alternatively, polymer assemblies can be kinetically trapped in a variety of morphologies. For example, spherical polymersomes composed of the amphiphilic block copolymer PEG-PS were subjected to a simultaneous dialysis and vitrification process which allowed the formation of more complex shapes such as disks or stomatocytes.⁶⁶

Mitragotri and colleagues have extensively studied the role of particle geometry on internalization using film-stretched PS-based micro- and nanoparticles with various aspect ratios (AR = width/height).^{63,67} They observed an aspect ratio-dependent, but size-independent uptake of particles by macrophages. When particle geometry is transformed from spherical to ellipsoidal to even filamentous, the aspect ratio increases

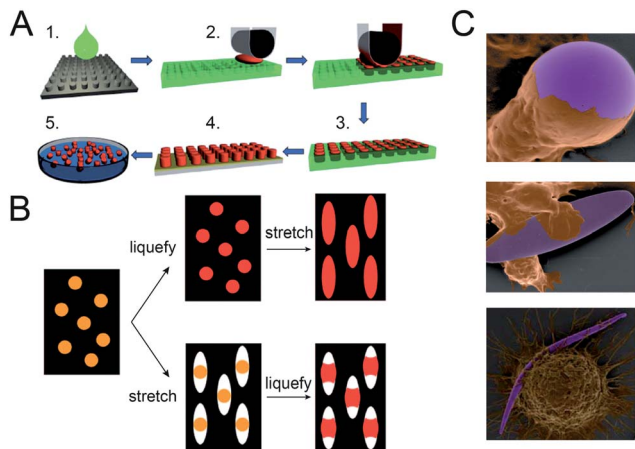


Fig. 5 (A) Preparation of particles using PRiNT. (1) An elastomeric PRiNT mold (green) is generated with micro/nanopatterns derived from the features on the silicon wafer. (2) A liquid pre-particle material (red) is filled into the mold. (3) The liquid is chemically converted into a solid. (4) Solid particles (red) can be removed from the mold by adding an adhesive layer (yellow) on top of the mold, which can pull particles from the mold. (5) Particles can be freed from the surface by dissolving the adhesive layer.⁶⁴ Reprinted from ref. 63. Copyright 2013 Wiley-VCH Verlag GmbH & Co. KGaA, Weinheim, Germany. (B) Preparation of particles from spherical particles using film-stretching. A dried film of particles is created, which can be stretched via two procedures: top: particles are first liquefied using heat or toluene, followed by film-stretching in one or two dimensions and solidification. Bottom: the film is first stretched in air to create voids around the particles, followed by liquefaction and finally solidification.⁶⁵ Copyright © 2007, The National Academy of Sciences. (C) Scanning electron microscopy of cells interacting with microparticles, brown = macrophages, purple = microparticles. Top: spherical particle being internalized by a macrophage. Middle: macrophage attaching and spreading the flat sides of a disk-shaped particle, but not internalizing it. Bottom: filamentous particles are not internalized by macrophages.^{65,67} Top and middle panel copyright © 2006, The National Academy of Sciences. Bottom panel reprinted with permission from ref. 62.

drastically ($AR = 1-20$) and particles are more likely to approach cells with their low curvature sides. As a result, ellipsoids showed more binding, but less uptake by macrophages than spherical particles, whereas the internalization of filamentous worms was completely inhibited (Fig. 5C).⁶⁷⁻⁶⁹

Importantly, when particles were functionalized with targeting ligands, elongated particles ($AR = 3-4$) displayed higher specific and lower non-specific uptake compared to spheres, which can likely be attributed to the large cell/ellipsoid contact area.⁷⁰ This finding was exploited by Doshi *et al.*, who developed phagocytosis-resistant PLGA-based constructs composed of flat disks (diameter 6 μm) covered with hemoglobin.⁵⁷

The advantage of using non-spherical particles as aAPC scaffold was recently shown by Sunshine *et al.*⁷¹ Ellipsoidal aAPCs exhibited more efficient *ex vivo* T-cell expansion than spherical aAPCs. This is probably caused by a combination of (1) reduced internalization and thus sustained T-cell signaling, and (2) an increased aAPC/T-cell contact area, which might enhance signaling strength.⁷¹ This hypothesis is in line with previous observations that microparticles are better at activating T-cells than nanoparticles,⁷² although this effect is not

always observed.⁵⁰ When ellipsoidal and spherical aAPCs were compared *in vivo*, ellipsoids induced a more potent anti-tumor response than spheres,⁷¹ yet it remains to be determined whether this is caused by differences in their interaction with T-cells or by a more favorable biodistribution.

T-cell ligand mobility

The ability of MHC-antigen complexes to relocate within the DC cell membrane in response to binding TCRs is crucial for IS formation and thus for efficient signal transduction.¹¹ Therefore, the dynamic remodeling of surface bound ligands on aAPCs is increasingly recognized as an important aspect in aAPC design. Although working with solid micro- and nanoparticles is appealing from an engineering point of view due to their high stability and reproducibility, these particles only allow for the random and fixed attachment of surface-bound ligands. Methods that allow for anisotropic or even dynamic surface presentation of T-cell recognition and costimulatory molecules can actively support IS formation, which will ultimately improve T-cell activation.

Using the PRiNT technology or particle masking, anisotropic or patterned microspheres have been prepared, consisting of PS particles coated with two proteins distributed into spatially separated domains.^{64,73} A polydimethylsiloxane (PDMS)-mask was created that shielded small circular patches from protein adsorption (Fig. 6A). After coupling the first protein, the protecting mask was removed and a second protein was selectively coupled to the patches, thereby creating patterned microparticles. This type of construct could be functionalized with T-cell ligands to create IS mimicking patches. Alternatively, poly(acrylic acid)/poly(allylamine hydrochloride) (PAA/PAH) microtubes have been prepared in which either the short ends or long sides contained hyaluronic acid, which strongly binds to cells.⁷⁴ This enabled orientation-specific attachment of particles to cells, which might be exploited to prevent particle internalization by directing preferred T-cell binding to the long sides.

However, these patterned constructs still lack ligand mobility. To create truly dynamic rearrangement of T-cell ligands on the aAPC surface, lipid-based aAPCs (liposomes) have been developed. Liposomes are spherical vesicles composed of a bilayer of amphiphilic lipids such as phosphatidyl-choline, -ethanolamine, -serine or cholesterol. The diffusion of individual lipids within this bilayer is dependent on the composition of the lipid mixture and the melting temperatures of individual lipids. The fluidic character of the bilayer allows for mechanical resizing, which is an advantage for *in vivo* applications of liposomes as aAPC.

Upon reconstitution of T-cell binding ligands into liposomes, these ligands can diffuse freely within the lipid bilayer.^{7,75-77} This unrestricted surface motility of T-cell ligands closely mimics natural DCs, as was shown by Prakken *et al.* who found that liposomes containing MHC class II-antigen complexes induced interfacial MHC/TCR clustering, thereby demonstrating the potential of signal clustering using lipid aAPCs.⁷⁵ For efficient T-cell activation though, preclustering of MHC-antigen and costimulatory antibodies within the lipid membranes was found to generate more efficient T-cell activation compared to homogeneously distributed ligands.⁷⁶ Signal

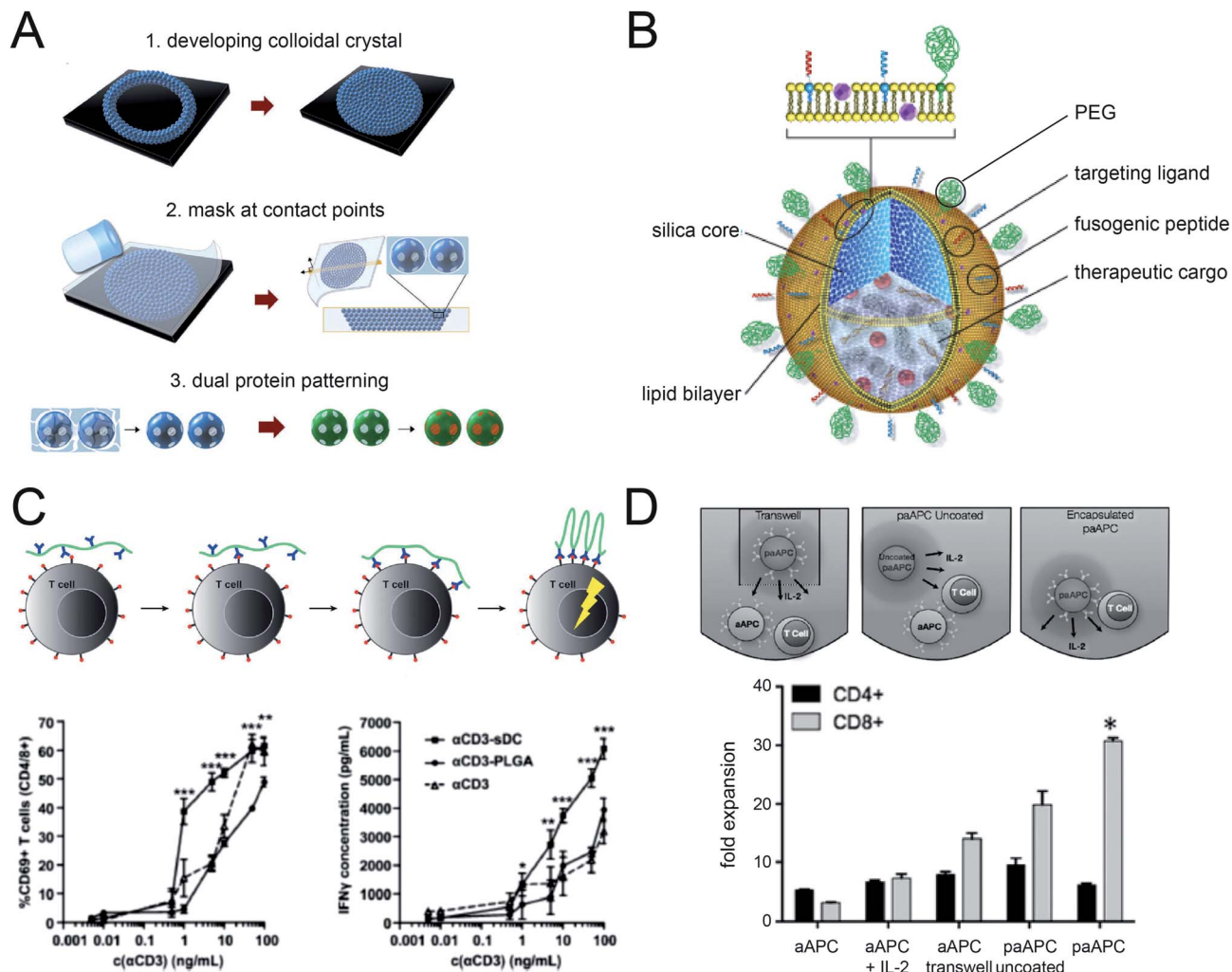


Fig. 6 (A) Production of anisotropically labeled microparticles. (1) Production colloidal crystals by iterative filling of colloidal well with microparticles. (2) Development of the mask at particle contact points. (3) Dual protein patterning. Microparticles are separated from the scaffold and labeled with the first protein (green) on the non-masked region. This is followed by removal of the mask and labeling with the second protein (red) on the previously masked regions.⁷³ Reprinted from ref. 72. Copyright 2011 Wiley-VCH Verlag GmbH & Co. KGaA, Weinheim, Germany. (B) Schematic overview of 3D supported lipid bilayer particles developed by Ashley *et al.* A lipid bilayer is deposited on a silica core that contains anti-cancer drugs. The lipid bilayer contains targeting ligands for efficient cancer cell binding, fusogenic peptides to facilitate particle uptake by cancer cells and PEG-tails to ultimately prolong the circulation time and thus enhanced tumor uptake.⁸¹ Reprinted by permission from Macmillan Publishers Ltd: *Nature Materials*, ref. 80, copyright 2011. (C) Top: proposed mechanism by which linear flexible polymeric aAPCs can facilitate IS formation and thus T-cell activation. Bottom: anti-CD3 polymers (SDC) are more efficient in T-cell activation than aCD3-PLGA microparticles or soluble anti-CD3.⁸⁴ Adapted from ref. 83 with permission from The Royal Society of Chemistry. (D) PLGA-based aAPCs containing signal 1 (anti-CD3), signal 2 (anti-CD28) and signal 3 (IL-2 release) require direct aAPC/T-cell contact to create local high IL-2 concentration to induce its stimulatory effect (right setup). Separation of IL-2 containing aAPCs (paAPC) and T-cells in a transwell system results in lower T-cell proliferation, even if anti-CD3/anti-CD28 aAPCs are added to the T-cell compartment (left setup). Also mixing of anti-CD3/anti-CD28 aAPCs and IL-2 particles (without anti-CD3/anti-CD28 coating) (middle scheme) results in less efficient T-cell activation compared to the three signal aAPC (paAPC).⁸⁹ This research was originally published in *Journal of Biological Chemistry*. Steenblock *et al.* An Artificial Antigen-presenting Cell with Paracrine Delivery of IL-2 Impacts the Magnitude and Direction of the T Cell Response. *Journal of Biological Chemistry*. 2011; **286**, 34883–92. © The American Society for Biochemistry and Molecular Biology.

clustering was achieved by incorporation of lipid raft-forming GM1-lipids, to which T-cell recognition and costimulatory antibodies were coupled, into the liposomes.⁷⁸ These preclustered, liposomal aAPCs were also compared with iron oxide microbeads for their ability to expand T-cells, showing that these nano-sized liposomes were as effective as microbeads, but preferentially expanded CD8⁺ over CD4⁺ T-cells, which is an advantage for *in vivo* induction of cytotoxic (CD8⁺) T-cells.⁷⁷

Liposomes have attractive features for the ideal aAPC system: they are biocompatible, biodegradable, have a membrane which is fluid enough for T-cell ligand reorganization and they allow for the incorporation of soluble immune-stimulating compounds. Unfortunately, their clinical use might ultimately be hampered by their poor stability, caused by lipid exchange between liposomes and cells. Polymersomes, prepared from amphiphilic block-co-polymers, may prove to be an attractive

alternative to liposomes.^{79,80} The individual polymer chains are longer than lipids, resulting in more rigid and stable particles, owing to the entanglement of the polymer chains at longer chain lengths and the higher melting points of polymers compared to lipids. A potential drawback of this increased stiffness is a reduced ligand mobility and a stringent size-dependent cut-off in the biodistribution, because of the inability of polymersomes to squeeze through small pores.⁸⁰

Another elegant solution is coating of solid nanoparticles with a lipid bilayer, so-called 3D SLBs.^{81–83} Cell-sized SLB have successfully been used for *in vitro* T-cell activation.⁸³ The lipid layer allows for lateral movement of surface bound ligands, to mimic the fluid nature of natural cell membranes, while the solid support provides stability *via* non-covalent interactions with lipids. The solid scaffold is usually composed of biodegradable PLGA or silica particles, thereby providing the attractive feature to include soluble active compounds within the particle core. For example, Ashley *et al.* developed silica-based SLB containing a cocktail of chemotherapeutic drugs that showed efficient tumor cell killing (Fig. 6B).⁸¹ Furthermore, they studied the influence of membrane fluidity on binding to cancer cells using lipids that are either above or below the melting point at 37 °C (DOPC and DPPC, respectively), thereby creating fluid or non-fluid SLB. As expected, increased membrane fluidity, and thus targeting ligand mobility, improved cancer cell binding.

Instead of using nano- or microparticles, an alternative aAPC concept was introduced by Mandal *et al.* (Fig. 6C).⁸⁴ In their aAPC design, a flexible linear isocyanide/dipeptide polymer was used as a backbone for T-cell ligand presentation. The isocyanide polymer adopts a helical structure in aqueous solvents, which is stabilized by linear sheets of hydrogen bonds between peptide side chains.⁸⁵ To these side chains, short PEG tails were attached to which T-cell ligands, in this case anti-CD3, were coupled. This polymer proved extremely potent in T-cell activation compared to PLGA-based microparticles, which were attributed to this aAPC's unique structure. Firstly, the isocyanide polymers appeared not to be internalized by T-cells, and therefore provide continuous receptor signaling. Secondly, the isocyanide polymer is flexible, thereby allowing for T-cell ligand repositioning upon T-cell binding. Finally, the spring-shaped backbone provides tension to the aAPC/T-cell binding sites, acting as an artificial cytoskeleton driving anti-CD3 clustering at the T-cell surface causing subsequent downstream signaling and activation.⁸⁶

Recently, Perica *et al.* provided an elegant example of induced ligand mobility with nano-sized (50–100 nm) iron-dextran-based aAPCs.⁸⁷ Although the ligands present on a single aAPC were immobile, the magnetic core of these particles allowed for an induced clustering effect of multiple aAPCs on the T-cell surface in the presence of a magnetic field. T-cells that were cultured with these aAPCs showed enhanced activation only in the presence of a magnetic field.

T-cell ligand conjugation

T-cells ligands can be attached to the surface of aAPCs *via* various linker strategies. When conjugating different types of T-cell ligands to a single construct it is desirable to have

control over coupling efficiency, stoichiometry and spatial arrangement. Fuertes *et al.* recently showed that especially when using non-specific coupling procedures to simultaneously conjugate multiple ligands, one ligand may outcompete binding of others.⁸⁸ By performing a stepwise coating strategy this direct competition can be overcome. It should however be noted that in a stepwise procedure the first ligand will occupy the more reactive and more sterically exposed positions on a given aAPC, which in turn could result in non-homogenous spatial distributions of different ligands. Therefore, Fuertes *et al.* rightly emphasize the need for quality-control of ligand conjugated aAPCs prior to their use in immunotherapy. Unfortunately, most studies do not address this issue of ligand coupling efficiencies, which makes comparisons of different types of aAPCs within a single study difficult and potentially misleading.

Many studies exploit non-covalent avidin–biotin interactions to functionalize avidin-coated particles with various biotinylated T-cell ligands.^{77,84,89} Theoretically, four biotin binding-sites are available per avidin molecule, which are stochastically filled with biotinylated proteins. Some authors claim the formation of preclustered microdomains composed of three different ligands (anti-CD3, anti-CD28 and anti-LFA-1) occupying a single avidin.^{76,77} However, statistically this is very unlikely in a single step incubation, and instead these three ligands will probably be randomly distributed over all the avidin molecules on the particles. Furthermore, full binding to all four available binding sites on avidin is rarely observed when coupling large biomolecules because of steric hindrance.

To gain more control over the coupling of multiple T-cell ligands onto a single aAPC scaffold, a combination of various more specific conjugation strategies can be used. When using lipid- or polymer-based particles, a variety of reactive end-groups can be employed for covalent linking of proteins *via* for example: maleimide–thiol, succinimidyl ester–amine or carbodiimide–carboxyl chemistries or bioorthogonal azide–alkyne/phosphine and Diels–Alder chemistries. When these chemistries are combined, particles can be functionalized with multiple ligands in a highly controlled manner using a different conjugation strategy for each type of ligand. A detailed discussion of this cross-linking chemistry is outside the scope of this review, but a recent review on this topic can be found elsewhere.⁹⁰

Even when applying orthogonal ligation chemistries for the introduction of different ligands onto aAPCs, a major challenge that will persist is to gain control over the distribution and orientation of these different functional groups on the aAPC's surface. On the biomolecule alike, control over the coupling position is important to retain its function. The standard amine, carboxylic acid and thiol chemistries that are mainly used to couple ligands can have dramatic influence on the integrity of active regions on these biomolecules and can also lead to suboptimal orientation of ligands on the surface of the aAPC, thereby rendering the ligands unavailable for T-cell activation. Therefore, the aAPC field could greatly benefit from advances in site-directed protein modification, both genetically^{91–93} and chemically (*e.g.* N-terminal diazotransfer)⁹⁴ and enzymatically (*e.g.* sortase).⁹⁵

Release of soluble ligands

Cytokine release allows cells to regulate processes in neighboring cells without the need for direct cell contact. A special class of cytokines, interleukins (IL), play an important role in the orchestration of the immune response generated upon DC/T-cell interactions. The ultimate T-cell phenotype is highly dependent on the type and local concentration of ILs that T-cells sense during DC-mediated activation.

In current *in vivo* applications of aAPCs, cytokines such as IL-2 are often administered systemically.^{45,50} However, this may lead to severe toxic side effects resulting from non-specific immune activation, a phenomenon known as cytokine storm.⁹⁶ Therefore, aAPC scaffolds that allow for controlled release of activating cytokines are highly desirable to enable high local concentrations, while avoiding systemic exposure.^{89,97–99} Traditionally, lipid nanoparticles and biodegradable polymeric solid particles have been used as localized delivery vehicles for anti-cancer or anti-inflammatory drugs.¹⁰⁰ Lipid nanoparticles allow for burst release of their contents, which can be either passively or actively regulated *e.g. via* the use of thermosensitive or pH-sensitive lipids.^{101,102} Alternatively, polymeric nanoparticles can be used that display a slower and more sustained release pattern upon polymer degradation, which can be achieved for example by using polymers with a hydrolysable backbone (*e.g.* PLGA) or side-groups (pHPMA).^{103,104} For PLGA, the rate of degradation can be tuned by adjusting the PLA/PGA ratio, thereby enabling local long-term steady cytokine concentrations, which might be preferred over the peak levels obtained by lipid particles.

The biodegradable polymer strategy was explored by Steenblock *et al.*, who developed PLGA-based microparticles that were surface-functionalized with both anti-CD3 and anti-CD28 and contained IL-2 encapsulated in the polymer matrix (Fig. 6D).^{72,89} The slow, sustained release of IL-2 from these microparticles significantly increased CD8⁺ T-cell proliferation in comparison with exogenously added IL-2. Furthermore, IL-2 release from the microparticles was required for efficient proliferation, as surface-bound IL-2 did not elicit an additional stimulatory effect. A possible limitation to these biodegradable systems is their intrinsic instability, which could limit the time that ligands are presented on the aAPC surface. However, Sunshine *et al.* showed that after one week incubation of PLGA particles at 37 °C, 30–40% of the targeting ligands were still present on the aAPC surface.⁷¹

Recently, Park *et al.* developed a novel drug delivery system composed of a lipid-bilayer covering a polymeric core, into which both hydrophilic and hydrophobic drugs can be loaded.⁹⁸ They used this scaffold for combined release of TGF- β inhibitors and IL-2 to counteract the immunosuppressive tumor micro-environment and simultaneously stimulate cytotoxic tumor-specific T-cells. With regards to aAPC design, this system possesses a unique combination of desired hallmarks. Its nano-size (100–150 nm) makes it extremely appealing for *in vivo* use. Furthermore, the polymer matrix allows for highly controllable cytokine release, whereas the lipid-coating facilitates surface-presentation of T-cell activating ligands, and allows for their mobility on the nanoparticle surface for improved IS formation.

In addition to immune-modulating cytokines, encapsulation of chemokines into aAPCs might also boost their T-cell activating function. Chemokines are cytokines that promote T-cell recruitment by creating cell-attracting signaling gradients. Upon their controlled release from particles, chemokines can actively attract T-cells towards these particles and thereby enhance aAPC/T-cell interactions. For example, *in vitro* release of CCL20 chemokine from PLGA particles enabled the recruitment of cells located at a distance up to 0.5 mm from the particles.¹⁰⁵ *In vivo*, CCL22-containing PLGA microparticles have been successfully used to recruit immune-suppressive T-cells to prevent local rejection of allogeneic cells.⁹⁹

Conclusions and outlook

Artificial antigen presenting cells as developed during the past decade show great potential to successfully mimic antigen-presentation to T-cells. Essential characteristics of natural T-cell activation have already been translated into simplified aAPC constructs, for example the dynamic remodeling of surface bound MHC–antigen complexes and co-stimulatory molecules in lipid bilayers to mimic an immune synapse. Also controlled delivery of immune modulating cytokines, such as IL-2, from for example biodegradable PLGA particles for T-cell differentiation has already been demonstrated. So far, most aAPCs have been used to stimulate and expand T-cells *in vitro*.

When moving towards aAPCs that support *in vivo* T-cell activation and expansion, a clear shift has been made from microparticles to nano-sized constructs, which are so small that they can passively accumulate in lymphoid organs where high numbers of T-cells reside. Ultimately, to move towards clinical application in cancer immunotherapy, a synthetic off-the-shelf aAPC system, which can be produced in bulk and subsequently loaded with tumor-antigens would be ideal. As such, aAPCs may develop into a widespread and powerful therapeutic tool that further expands the armory of immune intervention therapies that recently became available.

Acknowledgements

This work was supported by grants from the EU (ERC Advanced 'PATHFINDER' 269019) and the Dutch Government (Gravity Grants 'Institute for Chemical Immunology', Research Centre for Functional Molecular Systems' Gravity program 024.001.035), and (ChemTem 728.011.102). Carl Figdor received the NWO Spinoza Award.

Notes and references

- 1 J. Couzin-Frankel, *Science*, 2013, **342**, 1432–1433.
- 2 K. Palucka and J. Banchereau, *Nat. Rev. Cancer*, 2012, **12**, 265–277.
- 3 M. V. Maus, J. A. Fraietta, B. L. Levine, M. Kalos, Y. Zhao and C. H. June, *Annu. Rev. Immunol.*, 2014, 189–225.
- 4 C. H. June, B. R. Blazar and J. L. Riley, *Nat. Rev. Immunol.*, 2009, **9**, 704–716.

- 5 S. A. Rosenberg and M. E. Dudley, *Curr. Opin. Immunol.*, 2009, **21**, 233–240.
- 6 C. G. Figdor, I. J. M. de Vries, W. J. Lesterhuis and C. J. M. Melief, *Nat. Med.*, 2004, **10**, 475–480.
- 7 V. H. Engelhard, J. L. Strominger, M. Mescher and S. Burakoff, *Proc. Natl. Acad. Sci. U. S. A.*, 1978, **75**, 5688–5691.
- 8 E. R. Steenblock, S. H. Wrzesinski, R. A. Flavell and T. M. Fahmy, *Expert Opin. Biol. Ther.*, 2009, **9**, 451–464.
- 9 J. Xie, J. B. Huppa, E. W. Newell, J. Huang, P. J. R. Ebert, Q.-J. Li and M. M. Davis, *Nat. Immunol.*, 2012, **13**, 674–680.
- 10 M. F. Bachmann, K. McKall-Faienza, R. Schmits, D. Bouchard, J. Beach, D. E. Speiser, T. W. Mak and P. S. Ohashi, *Immunity*, 1997, **7**, 549–557.
- 11 C. R. Monks, B. A. Freiberg, H. Kupfer, N. Sciaky and A. Kupfer, *Nature*, 1998, **395**, 82–86.
- 12 M. L. Dustin and J. T. Groves, *Annu. Rev. Biophys.*, 2012, **41**, 543–556.
- 13 D. J. Irvine, M. A. Purbhoo, M. Krogsgaard and M. M. Davis, *Nature*, 2002, **419**, 845–849.
- 14 J. P. Van Wauwe, J. R. De Mey and J. G. Goossens, *J. Immunol.*, 1980, **124**, 2708–2713.
- 15 S. C. Meuer, *J. Exp. Med.*, 1983, **158**, 988–993.
- 16 L. Zhou, M. M. W. Chong and D. R. Littman, *Immunity*, 2009, **30**, 646–655.
- 17 A. Grakoui, S. K. Bromley, C. Sumen, M. M. Davis, A. S. Shaw, P. M. Allen and M. L. Dustin, *Science*, 1999, **285**, 221–227.
- 18 D. J. Irvine and J. Doh, *Semin. Immunol.*, 2007, **19**, 245–254.
- 19 M. J. P. Biggs, M. C. Milone, L. C. Santos, A. Gondarenko and S. J. Wind, *J. R. Soc., Interface*, 2011, **8**, 1462–1471.
- 20 Y. Kaizuka, A. D. Douglass, R. Varma, M. L. Dustin and R. D. Vale, *Proc. Natl. Acad. Sci. U. S. A.*, 2007, **104**, 20296–20301.
- 21 K. Choudhuri, J. Llodrá, E. W. Roth, J. Tsai, S. Gordo, K. W. Wucherpfennig, L. C. Kam, D. L. Stokes and M. L. Dustin, *Nature*, 2014, **507**, 118–123.
- 22 K. D. Mossman, G. Campi, J. T. Groves and M. L. Dustin, *Science*, 2005, **310**, 1191–1193.
- 23 K. Shen, J. Tsai, P. Shi and L. C. Kam, *J. Am. Chem. Soc.*, 2009, **131**, 13204–13205.
- 24 J. Doh and D. J. Irvine, *Proc. Natl. Acad. Sci. U. S. A.*, 2006, **103**, 5700–5705.
- 25 C.-J. Hsu, W.-T. Hsieh, A. Waldman, F. Clarke, E. S. Huseby, J. K. Burkhardt and T. Baumgart, *PLoS One*, 2012, **7**, e32398.
- 26 J. Rossy, S. V. Pigeon, D. M. Davis and K. Gaus, *Curr. Opin. Immunol.*, 2013, **25**, 307–312.
- 27 N. K. Garlie, A. V. LeFever, R. E. Siebenlist, B. L. Levine, C. H. June and L. G. Lum, *J. Immunother.*, 1999, **22**, 336–345.
- 28 F. Ito, A. Carr, H. Svensson, J. Yu, A. E. Chang and Q. Li, *J. Immunother.*, 2003, **26**, 222–233.
- 29 M. F. Mescher, *J. Immunol.*, 1992, **149**, 2402–2405.
- 30 D. L. Porter, B. L. Levine, M. Kalos, A. Bagg and C. H. June, *N. Engl. J. Med.*, 2011, **365**, 725–733.
- 31 L. G. Lum, A. V. LeFever, J. S. Treisman, N. K. Garlie and J. P. Hanson, *J. Immunother.*, 2001, **24**, 408–419.
- 32 G. G. Laport, B. L. Levine, E. A. Stadtmauer, S. J. Schuster, S. M. Luger, S. Grupp, N. Bunin, F. J. Strobl, J. Cotte, Z. Zheng, B. Gregson, P. Rivers, R. H. Vonderheide, D. N. Liebowitz, D. L. Porter and C. H. June, *Blood*, 2003, **102**, 2004–2013.
- 33 N. M. Hardy, M. E. Mossoba, S. M. Steinberg, V. Fellowes, X.-Y. Yan, F. T. Hakim, R. R. Babb, D. Avila, J. Gea-Banacloche, C. Sportès, B. L. Levine, C. H. June, H. M. Khuu, A. E. Carpenter, M. C. Krumlauf, A. J. Dwyer, R. E. Gress, D. H. Fowler and M. R. Bishop, *Clin. Cancer Res.*, 2011, **17**, 6878–6887.
- 34 M. V. Maus, J. L. Riley, W. W. Kwok, G. T. Nepom and C. H. June, *Clin. Immunol.*, 2003, **106**, 16–22.
- 35 M. Oelke, M. V. Maus, D. Didiano, C. H. June, A. Mackensen and J. P. Schneck, *Nat. Med.*, 2003, **9**, 619–624.
- 36 K. Schilbach, G. Kerst, S. Walter, M. Eylich, D. Wernet, R. Handgretinger, W. Xie, H.-G. Rammensee, I. Müller, H.-J. Bühring and D. Niethammer, *Blood*, 2005, **106**, 144–149.
- 37 C. P. Broeren, G. S. Gray, B. M. Carreno and C. H. June, *J. Immunol.*, 2000, **165**, 6908–6914.
- 38 M. J. Deeths and M. F. Mescher, *Eur. J. Immunol.*, 1999, **29**, 45–53.
- 39 D. Rudolf, T. Silberzahn, S. Walter, D. Maurer, J. Engelhard, D. Wernet, H.-J. Bühring, G. Jung, B. S. Kwon, H.-G. Rammensee and S. Stevanović, *Cancer Immunol. Immunother.*, 2008, **57**, 175–183.
- 40 M. J. Deeths and M. F. Mescher, *Eur. J. Immunol.*, 1997, **27**, 598–608.
- 41 M. Durai, C. Krueger, Z. Ye, L. Cheng, A. Mackensen, M. Oelke and J. P. Schneck, *Cancer Immunol. Immunother.*, 2009, **58**, 209–220.
- 42 X. Lu, X. Jiang, R. Liu, H. Zhao and Z. Liang, *Cancer Lett.*, 2008, **271**, 129–139.
- 43 C. Shen, K. Cheng, S. Miao, W. Wang, Y. He, F. Meng and J. Zhang, *Immunol. Lett.*, 2013, **150**, 1–11.
- 44 S. Caserta, P. Alessi, J. Guarnerio, V. Basso and A. Mondino, *Cancer Res.*, 2008, **68**, 3010–3018.
- 45 S. Ugel, A. Zoso, C. De Santo, Y. Li, I. Marigo, P. Zanovello, E. Scarselli, B. Cipriani, M. Oelke, J. P. Schneck and V. Bronte, *Cancer Res.*, 2009, **69**, 9376–9384.
- 46 N. Bertrand and J.-C. Leroux, *J. Controlled Release*, 2012, **161**, 152–163.
- 47 P. Decuzzi, B. Godin, T. Tanaka, S. Y. Lee, C. Chiappini, X. Liu and M. Ferrari, *J. Controlled Release*, 2010, **141**, 320–327.
- 48 S. T. Reddy, A. Rehor, H. G. Schmoekel, J. A. Hubbell and M. A. Swartz, *J. Controlled Release*, 2006, **112**, 26–34.
- 49 V. Manolova, A. Flace, M. Bauer, K. Schwarz, P. Saudan and M. F. Bachmann, *Eur. J. Immunol.*, 2008, **38**, 1404–1413.
- 50 K. Perica, A. De León Medero, M. Durai, Y. L. Chiu, J. G. Bieler, L. Sibener, M. Niemöller, M. Assenmacher, A. Richter, M. Edidin, M. Oelke and J. Schneck, *Nanomedicine*, 2014, **10**, 119–129.
- 51 C. Oussoren, J. Zuidema, D. J. A. Crommelin and G. Storm, *Biochim. Biophys. Acta, Biomembr.*, 1997, **1328**, 261–272.
- 52 R. A. Petros and J. M. DeSimone, *Nat. Rev. Drug Discovery*, 2010, **9**, 615–627.

- 53 L. E. Paulis, S. Mandal, M. Kreutz and C. G. Figdor, *Curr. Opin. Immunol.*, 2013, **25**, 389–395.
- 54 J. A. Champion, Y. K. Katare and S. Mitragotri, *J. Controlled Release*, 2007, **121**, 3–9.
- 55 Y. Geng, P. Dalhaimer, S. Cai, R. Tsai, M. Tewari, T. Minko and D. E. Discher, *Nat. Nanotechnol.*, 2007, **2**, 249–255.
- 56 T. J. Merkel, S. W. Jones, K. P. Herlihy, F. R. Kersey, A. R. Shields, M. Napier, J. C. Luft, H. Wu, W. C. Zamboni, A. Z. Wang, J. E. Bear and J. M. DeSimone, *Proc. Natl. Acad. Sci. U. S. A.*, 2011, **108**, 586–591.
- 57 N. Doshi, A. S. Zahr, S. Bhaskar, J. Lahann and S. Mitragotri, *Proc. Natl. Acad. Sci. U. S. A.*, 2009, **106**, 21495–21499.
- 58 R. Gref, Y. Minamitake, M. Peracchia, V. Trubetsky, V. Torchilin and R. Langer, *Science*, 1994, **263**, 1600–1603.
- 59 K. Knop, R. Hoogenboom, D. Fischer and U. S. Schubert, *Angew. Chem., Int. Ed.*, 2010, **49**, 6288–6308.
- 60 P. L. Rodriguez, T. Harada, D. A. Christian, D. A. Pantano, R. K. Tsai and D. E. Discher, *Science*, 2013, **339**, 971–975.
- 61 C. M. Jewell, S. C. B. López and D. J. Irvine, *Proc. Natl. Acad. Sci. U. S. A.*, 2011, **108**, 15745–15750.
- 62 M. J. Miller, O. Safrina, I. Parker and M. D. Cahalan, *J. Exp. Med.*, 2004, **200**, 847–856.
- 63 J. A. Champion and S. Mitragotri, *Pharm. Res.*, 2009, **26**, 244–249.
- 64 J. Xu, D. H. C. Wong, J. D. Byrne, K. Chen, C. Bowerman and J. M. DeSimone, *Angew. Chem., Int. Ed.*, 2013, **52**, 6580–6589.
- 65 J. A. Champion, Y. K. Katare and S. Mitragotri, *Proc. Natl. Acad. Sci. U. S. A.*, 2007, **104**, 11901–11904.
- 66 K. T. Kim, J. Zhu, S. A. Meeuwissen, J. J. L. M. Cornelissen, D. J. Pochan, R. J. M. Nolte and J. C. M. van Hest, *J. Am. Chem. Soc.*, 2010, **132**, 12522–12524.
- 67 J. A. Champion and S. Mitragotri, *Proc. Natl. Acad. Sci. U. S. A.*, 2006, **103**, 4930–4934.
- 68 J. A. Champion, A. Walker and S. Mitragotri, *Pharm. Res.*, 2008, **25**, 1815–1821.
- 69 G. Sharma, D. T. Valenta, Y. Altman, S. Harvey, H. Xie, S. Mitragotri and J. W. Smith, *J. Controlled Release*, 2010, **147**, 408–412.
- 70 S. Barua, J.-W. Yoo, P. Kolhar, A. Wakankar, Y. R. Gokarn and S. Mitragotri, *Proc. Natl. Acad. Sci. U. S. A.*, 2013, **110**, 3270–3275.
- 71 J. C. Sunshine, K. Perica, J. P. Schneck and J. J. Green, *Biomaterials*, 2014, **35**, 269–277.
- 72 E. R. Steenblock and T. M. Fahmy, *Mol. Ther.*, 2008, **16**, 765–772.
- 73 K. Kamalasanan, S. Jhunjunwala, J. Wu, A. Swanson, D. Gao and S. R. Little, *Angew. Chem., Int. Ed.*, 2011, **50**, 8706–8708.
- 74 J. B. Gilbert, J. S. O'Brien, H. S. Suresh, R. E. Cohen and M. F. Rubner, *Adv. Mater.*, 2013, **25**, 5948–5952.
- 75 B. Prakken, M. Wauben, D. Genini, R. Samodal, J. Barnett, A. Mendivil, L. Leoni and S. Albani, *Nat. Med.*, 2000, **6**, 1406–1410.
- 76 F. Giannoni, J. Barnett, K. Bi, R. Samodal, P. Lanza, P. Marchese, W. W. Kwok, E. Sercarz, A. Altman and S. Albani, *J. Immunol.*, 2005, **174**, 3204–3211.
- 77 R. Zappasodi, M. Di Nicola, C. Carlo-Stella, R. Mortarini, A. Molla, C. Vegetti, S. Albani, A. Anichini and A. M. Gianni, *Haematologica*, 2008, **93**, 1523–1534.
- 78 C. Yuan, J. Furlong, P. Burgos and L. J. Johnston, *Biophys. J.*, 2002, **82**, 2526–2535.
- 79 B. M. Discher, Y.-Y. Won, D. S. Ege, J. C.-M. Lee, F. S. Bates, D. E. Discher and D. A. Hammer, *Science*, 1999, **284**, 1143–1146.
- 80 R. P. Brinkhuis, F. P. J. T. Rutjes and J. C. M. van Hest, *Polym. Chem.*, 2011, **2**, 1449.
- 81 C. E. Ashley, E. C. Carnes, G. K. Phillips, D. Padilla, P. N. Durfee, P. A. Brown, T. N. Hanna, J. Liu, B. Phillips, M. B. Carter, N. J. Carroll, X. Jiang, D. R. Dunphy, C. L. Willman, D. N. Petsev, D. G. Evans, A. N. Parikh, B. Chackerian, W. Wharton, D. S. Peabody and C. J. Brinker, *Nat. Mater.*, 2011, **10**, 389–397.
- 82 T. Jin, P. Pennefather and P. I. Lee, *FEBS Lett.*, 1996, **397**, 70–74.
- 83 S. A. Goldstein and M. F. Mescher, *J. Immunol.*, 1986, **137**, 3383–3392.
- 84 S. Mandal, Z. H. Eksteen-Akeroyd, M. J. Jacobs, R. Hammink, M. Koepf, A. J. A. Lambeck, J. C. M. van Hest, C. J. Wilson, K. Blank, C. G. Figdor and A. E. Rowan, *Chem. Sci.*, 2013, **4**, 4168.
- 85 J. J. Cornelissen, J. J. Donners, R. de Gelder, W. S. Graswinckel, G. A. Metselaar, A. E. Rowan, N. A. Sommerdijk and R. J. Nolte, *Science*, 2001, **293**, 676–680.
- 86 E. Judokusumo, E. Tabdanov, S. Kumari, M. L. Dustin and L. C. Kam, *Biophys. J.*, 2012, **102**, L5–L7.
- 87 K. Perica, A. Tu, A. Richter, J. G. Bieler, M. Edidin and J. P. Schneck, *ACS Nano*, 2014, **8**, 2252–2260.
- 88 S. A. Fuertes Marraco, P. Baumgaertner, A. Legat, N. Rufer and D. E. Speiser, *J. Immunol. Methods*, 2012, **385**, 90–95.
- 89 E. R. Steenblock, T. Fadel, M. Labowsky, J. S. Pober and T. M. Fahmy, *J. Biol. Chem.*, 2011, **286**, 34883–34892.
- 90 W. R. Algar, D. E. Prasuhn, M. H. Stewart, T. L. Jennings, J. B. Blanco-Canosa, P. E. Dawson and I. L. Medintz, *Bioconjugate Chem.*, 2011, **22**, 825–858.
- 91 A. J. Link, M. L. Mock and D. A. Tirrell, *Curr. Opin. Biotechnol.*, 2003, **14**, 603–609.
- 92 J. W. Chin, T. A. Cropp, J. C. Anderson, M. Mukherji, Z. Zhang and P. G. Schultz, *Science*, 2003, **301**, 964–967.
- 93 J. W. Chin, *Science*, 2012, **336**, 428–429.
- 94 S. F. M. van Dongen, R. L. M. Teeuwen, M. Nallani, S. S. van Berkel, J. J. L. M. Cornelissen, R. J. M. Nolte and J. C. M. van Hest, *Bioconjugate Chem.*, 2009, **20**, 20–23.
- 95 C. S. Theile, M. D. Witte, A. E. M. Blom, L. Kundrat, H. L. Ploegh and C. P. Guimaraes, *Nat. Protoc.*, 2013, **8**, 1800–1807.
- 96 J. P. Siegel and R. K. Puri, *J. Clin. Oncol.*, 1991, **9**, 694–704.
- 97 J. Park, W. Gao, R. Whiston, T. B. Strom, S. Metcalfe and T. M. Fahmy, *Mol. Pharm.*, 2011, **8**, 143–152.

- 98 J. Park, S. H. Wrzesinski, E. Stern, M. Look, J. Criscione, R. Ragheb, S. M. Jay, S. L. Demento, A. Agawu, P. Licon Limon, A. F. Ferrandino, D. Gonzalez, A. Habermann, R. A. Flavell and T. M. Fahmy, *Nat. Mater.*, 2012, **11**, 895–905.
- 99 S. Jhunjhunwala, S. C. Balmert, G. Raimondi, E. Dons, E. E. Nichols, A. W. Thomson and S. R. Little, *J. Controlled Release*, 2012, **159**, 78–84.
- 100 J. M. Metselaar and G. Storm, *Expert Opin. Drug Delivery*, 2005, **2**, 465–476.
- 101 M. de Smet, S. Langereis, S. van den Bosch and H. Grüll, *J. Controlled Release*, 2010, **143**, 120–127.
- 102 E. Yuba, Y. Kono, A. Harada, S. Yokoyama, M. Arai, K. Kubo and K. Kono, *Biomaterials*, 2013, **34**, 5711–5721.
- 103 L. J. Cruz, P. J. Tacke, R. Fokkink, B. Joosten, M. C. Stuart, F. Albericio, R. Torensma and C. G. Figdor, *J. Controlled Release*, 2010, **144**, 118–126.
- 104 M. Talelli, C. J. F. Rijcken, C. F. van Nostrum, G. Storm and W. E. Hennink, *Adv. Drug Delivery Rev.*, 2010, **62**, 231–239.
- 105 X. Zhao, S. Jain, H. Benjamin Larman, S. Gonzalez and D. J. Irvine, *Biomaterials*, 2005, **26**, 5048–5063.
- 106 L. E. Paulis, T. Geelen, M. T. Kuhlmann, B. F. Coolen, M. Schäfers, K. Nicolay and G. J. Strijkers, *J. Controlled Release*, 2012, **162**, 276–285.